BIOCHEMISTRY
including biophysical chemistry & molecular biology
Article

Biochemistry **2010,** *49,* 5743–5752 5743
DOI: 10.1021/bi100618g

Reconstitution of *Helicobacter pylori* VacA Toxin from Purified Components†

Christian González-Rivera,‡,@ Kelly A. Gangwer,‡,@ Mark S. McClain,§ Ilyas M. Eli,∥ Melissa G. Chambers,∥ Melanie D. Ohi,∥ D. Borden Lacy,*,‡ and Timothy L. Cover*,‡,§,⊥

‡*Department of Microbiology and Immunology,* §*Department of Medicine, and* ∥*Department of Cell and Developmental Biology, Vanderbilt University School of Medicine, Nashville, Tennessee 37232, and* ⊥*Veterans Affairs Tennessee Valley Healthcare System, Nashville, Tennessee 37212.* @*These authors contributed equally to this work.*

Received April 22, 2010; Revised Manuscript Received June 6, 2010

ABSTRACT: *Helicobacter pylori* VacA is a pore-forming toxin that causes multiple alterations in human cells and contributes to the pathogenesis of peptic ulcer disease and gastric cancer. The toxin is secreted by *H. pylori* as an 88 kDa monomer (p88) consisting of two domains (p33 and p55). While an X-ray crystal structure for p55 exists and p88 oligomers have been visualized by cryo-electron microscopy, a detailed analysis of p33 has been hindered by an inability to purify this domain in an active form. In this study, we expressed and purified a recombinant form of p33 under denaturing conditions and optimized conditions for the refolding of the soluble protein. We show that refolded p33 can be added to purified p55 in trans to cause vacuolation of HeLa cells and inhibition of IL-2 production by Jurkat cells, effects identical to those produced by the p88 toxin from *H. pylori*. The p33 protein markedly enhances the cell binding properties of p55. Size exclusion chromatography experiments suggest that p33 and p55 assemble into a complex consistent with the size of a p88 monomer. Electron microscopy of these p33/p55 complexes reveals small rod-shaped structures that can convert to oligomeric flower-shaped structures in the presence of detergent. We propose that the oligomerization observed in these experiments mimics the process by which VacA oligomerizes when in contact with membranes of host cells.

Helicobacter pylori is a Gram-negative bacterium that persistently colonizes the human stomach (*1*−*4*). Infection by *H. pylori* is associated with the development of peptic ulcer disease, gastric adenocarcinoma, and gastric lymphoma (*5*, *6*). An important virulence factor in the pathogenesis of *H. pylori* infection is a secreted protein known as vacuolating cytotoxin (VacA) (*7*−*11*). In vivo studies have shown that VacA contributes to gastric damage in animal models (*12*, *13*), and specific *vacA* allelic forms are associated with an increased risk of disease in humans (*14*, *15*). VacA causes a wide range of cellular alterations in vitro (*9*), including the formation of large cytoplasmic vacuoles (*7*, *8*), permeabilization of the plasma membrane (*16*), reduction of mitochondrial transmembrane potential and cytochrome *c* release (*17*, *18*), activation of mitogen-activated protein kinases (*19*), induction of autophagy (*20*), and inhibition of the activation and proliferation of T-lymphocytes (*21*−*23*). Many cellular effects of VacA are dependent on the formation of anion-selective membrane channels (*9*, *16*, *24*, *25*). VacA-induced cell vacuolation, the hallmark effect of VacA on epithelial cells, results from internalization of VacA and expansion of late endosomal compartments (*9*, *26*). VacA-induced suppression of IL-2 production, a prominent effect of VacA on Jurkat T cells, is attributed to inhibited nuclear translocation of NFAT (*21*).

The *vacA* gene encodes a 140 kDa protein that undergoes proteolytic processing to yield an amino-terminal signal sequence, an 88 kDa secreted toxin, and a carboxyl-terminal autotransporter domain (*13*, *27*−*29*). Partial proteolytic digestion in vitro of the 88 kDa secreted toxin yields two fragments, designated p33 and p55, which probably represent two domains of VacA (*13*, *30*−*32*). Cleavage of the p88 protein into these two fragments occurs at a site that is predicted to be a surface-exposed flexible loop (*13*, *31*). Amino acid sequences within an amino-terminal hydrophobic portion of the p33 domain are required for membrane channel formation (*33*, *34*), and sequences within the p55 domain are required for VacA binding to cells (*35*−*37*). When expressed intracellularly in HeLa cells, ∼422 residues (corresponding to the p33 domain and the amino-terminal portion of the p55 domain) are sufficient to cause cell vacuolation (*38*). Intracellularly expressed p33 localizes in association with mitochondria, whereas p55 does not (*17*). The crystal structure of p55 was recently analyzed and shown to consist predominantly of a right-handed parallel β-helix (*39*), a property that is shared among most autotransporter passenger domains (*39*−*41*). It is predicted that a large portion of p33 also comprises a β-helical fold (*39*), but thus far, detailed studies of p33 have been hindered by an inability to purify an active form of this domain.

The 88 kDa VacA monomers secreted by *H. pylori* can assemble into large water-soluble oligomeric complexes (*42*−*45*). These flower-shaped structures can be either single-layer (containing 6−9 subunits) or bilayer (containing 12−14 subunits) (*42*−*45*).

†This work was supported by the National Institutes of Health (Grant R01AI39657), the Department of Veterans Affairs, the Burroughs Wellcome Fund, the Molecular Microbial Pathogenesis Training Program (T32 AI007281-21), the Molecular Biophysics Training Program (T32 GM08320), and Vanderbilt Development funds.

*To whom correspondence should be addressed. T.L.C.: Division of Infectious Diseases, A2200 Medical Center North, Vanderbilt University School of Medicine, Nashville, TN 37232; phone, (615) 322-2035; fax, (615) 343-6160; e-mail, timothy.L.cover@vanderbilt.edu. D.B.L.: Department of Microbiology and Immunology, Vanderbilt University School of Medicine, Nashville, TN 37232; phone, (615) 343-9080; fax, (615) 936-2211; e-mail, borden.lacy@vanderbilt.edu.

Published on Web 06/08/2010

Similar oligomeric structures have been visualized on the surface of VacA-treated cells or lipid bilayers (*24*, *44*, *46*). Amino acid sequences within both the p33 domain (residues 49−57) and the p55 domain (residues 346 and 347) are required for assembly of VacA into these oligomeric structures, and mutant proteins lacking these sequences fail to cause cell vacuolation (*47*, *48*). Several VacA mutant proteins have dominant negative inhibitory effects on the ability of wild-type VacA to cause cellular alterations (*33*, *48*−*50*), which supports the hypothesis that oligomeric structures are required for VacA effects on host cells. Water-soluble VacA oligomeric complexes lack cytotoxic activity unless they are first dissociated into monomeric components by exposure to low-pH or high-pH conditions (*42*, *51*), and therefore, it is presumed that VacA monomeric components interact with host cells and subsequently reassemble into membrane channels. Although the structure of water-soluble VacA oligomeric complexes has been investigated in detail, the conditions that promote oligomerization of VacA are not well-understood.

In this study, we describe the expression and purification of a recombinant form of p33 that, when mixed with p55, causes cellular alterations identical to those caused by p88 VacA from *H. pylori*. We report that p33 and p55 assemble into a complex consistent with the size of a p88 monomer, and that p33 markedly enhances the cell binding properties of p55. Furthermore, we report that, in the presence of detergent, p33 and p55 assemble into oligomeric structures that resemble the oligomeric complexes formed by p88 VacA from *H. pylori*. We discuss the importance of this assembly in the process by which VacA intoxicates human cells, and in addition, we discuss the distinctive structural properties of VacA that allow reconstitution of a functional protein from two individually expressed component domains.

EXPERIMENTAL PROCEDURES

Purification of p88 VacA from the H. pylori Broth Culture Supernatant. *H. pylori* strain 60190 (expressing wild-type VacA) and a strain expressing a VacAΔ6−27 mutant protein were grown in broth culture, and VacA proteins were purified in an oligomeric form from the culture supernatant as described previously (*33*, *42*). These preparations of purified VacA oligomers were acid-activated prior to use in cell culture experiments (*42*, *51*).

Plasmids for Expression of p33 and p55 VacA Fragments. Plasmids encoding the p33 and p55 domains of VacA from *H. pylori* strain 60190 (a type s1/m1 form of VacA; GenBank accession number Q48245), as well as a c-Myc-tagged p33 protein and a p33Δ6−27 mutant protein, have been described previously (*27*, *32*, *39*, *49*). The p33 proteins contain a C-terminal hexahistidine tag, and the p55 protein contains an N-terminal hexahistidine tag.

Expression and Purification of Recombinant VacA Proteins. VacA p55 was purified as described previously (*39*). VacA p33 was expressed in *Escherichia coli* BL21(DE3) by culturing in Terrific broth (Fisher) supplemented with 25 μg/mL kanamycin (TB-KAN)[1] at 37 °C overnight with shaking. A c-Myc-tagged form of p33 (*32*) was expressed in the same manner. Cultures were diluted 1:100 in TB-KAN and grown at 37 °C until they reached an absorbance (A_{600}) of 0.6. Cultures were induced with a final isopropyl β-D-thiogalactopyranoside (IPTG) concentration of 0.5 mM and incubated at 37 °C for 2 h.

VacA p33 proteins were purified from inclusion bodies. Briefly, IPTG-induced cultures were pelleted, washed in 0.9% NaCl, and resuspended (10 mL/L of culture) in sonication buffer [10 mM Tris (pH 7.5), 100 mM NaCl, 1 mM EDTA, protease inhibitor (Roche), and 20000 units/mL lysozyme (Ready-lyse, Epicenter)]. The cells were incubated at room temperature for 15 min with shaking and sonicated with six 20 W bursts (45 s per burst with 15 s cooling periods). Lysed bacterial cells were centrifuged to pellet the inclusion bodies. The insoluble inclusion body pellet was resuspended in buffer containing 100 mM NaH_2PO_4, 10 mM Tris, and 8 M urea (pH 8.0) at 5 mL/g of wet weight and incubated for 1 h at room temperature. The samples were centrifuged, and the resulting supernatant was added to Ni-NTA beads (Novagen) at a ratio of 4 mL of supernatant/mL of beads. The protein/bead mixture was incubated for 1 h at room temperature before being loaded into a column. The column was washed with 10 column volumes of 100 mM NaH_2PO_4, 10 mM Tris, 10 mM imidazole, and 8 M urea (pH 6.3), followed by 100 mM NaH_2PO_4, 10 mM Tris, and 8 M urea (pH 5.9). The p33 protein was eluted from the column with 100 mM NaH_2PO_4, 10 mM Tris, and 8 M urea (pH 4.5). Successful expression and purification of p33 were confirmed by mass spectrometry (data not shown).

Refolding of VacA p33. The denatured VacA p33 protein was refolded via dialysis of the protein against a buffer containing 55 mM Tris, 21 mM NaCl, 0.88 mM KCl, 1.1 M guanidine, and 880 mM arginine (pH 8.2) for 24 h. The protein then was dialyzed in two other buffers, each for 24 h. The first reduced the guanidine concentration to 800 mM and the arginine concentration to 500 mM, and the second reduced the arginine concentration to 250 mM and maintained a guanidine concentration of 800 mM (*52*). Further reductions in the arginine or guanidine concentrations resulted in precipitation of p33 VacA.

Cell Culture Assays. HeLa cells were grown in minimal essential medium (modified Eagle's medium containing Earle's salts) supplemented with 10% fetal bovine serum (FBS) in a 5% CO_2 atmosphere at 37 °C. Jurkat lymphocytes (clone E6-1) (ATCC TIB-152) were grown in RPMI 1640 medium containing 2 mM L-glutamine, 1.5 g/L sodium bicarbonate, 4.5 g/L glucose, 10 mM HEPES, and 1.0 mM sodium pyruvate supplemented with 10% FBS.

For vacuolating assays, HeLa cells were seeded at a density of 1.2×10^4 cells/well into 96-well plates 24 h prior to the addition of VacA proteins. The recombinant p33 and p55 proteins (each at 1 mg/mL) were premixed in a 1:1 mass ratio, which corresponds to an ~1.7:1 molar ratio. The use of excess p33 on a molar basis compensated for the possibility that refolding of denatured p33 might be less than 100% efficient. Preparations of purified p33, p55, or the p33/p55 mixture were then added to the tissue culture medium overlying HeLa cells (supplemented with 10 mM ammonium chloride) and incubated overnight at 37 °C. VacA-induced cell vacuolation was detected by inverted light microscopy and quantified by a neutral red uptake assay, a well-established method that is based on rapid uptake of neutral red into VacA-induced cell vacuoles (*8*, *53*). For dominant negative assays, we tested the ability of the refolded p33Δ6−27 protein or the purified *H. pylori* p88 Δ6−27 protein to inhibit the activity of wild-type VacA (*33*, *49*). To analyze VacA effects on T cells, we analyzed the capacity of VacA to inhibit IL-2 secretion by Jurkat

[1]Abbreviations: NFAT, nuclear factor of activated T cells; TB-KAN, Terrific broth containing kanamycin; IPTG, isopropyl β-D-thiogalactopyranoside; PMA, phorbol 12-myristate 13-acetate; FBS, fetal bovine serum; EM, electron microscopy; DDM, *n*-dodecyl β-D-maltoside; mrc, mixed raster content.

T cells (*21*) . Jurkat cells were plated at a density of 1×10^5 cells/well, and recombinant p33 and p55 were added to cells either individually or as a p33/p55 mixture (1:1 mass ratio) for 30 min at 37 °C. After incubation, 0.05 μg/mL phorbol 12-myristate 13-acetate (PMA) and 0.5 μg/mL ionomycin were added for 24 h at 37 °C. The cells were then centrifuged at 2000 rpm for 7 min, and the supernatants were tested for IL-2 by an ELISA, according to the manufacturer's protocol (R&D Systems Human IL-2 Immunoassay) (*54*).

Interactions of p33 and p55 with HeLa Cells. Purified p55 was labeled with Alexa 488 (Molecular Probes) according to the manufacturer's instructions. HeLa cells were incubated with Alexa 488-labeled p55 alone (10 μg/mL) or a mixture of labeled p55 with purified refolded p33 (each at 5 μg/mL) at 37 °C. Alternatively, cells were incubated with purified Alexa 488-labeled p55 with a c-Myc-tagged p33 protein (*32*) that was purified and refolded using the same methodology described above for p33. Cells were fixed with 4% formaldehyde. The c-Myc-tagged p33 protein was detected by indirect immunofluorescence using an anti-c-Myc antibody and an Alexa fluor-555-conjugated secondary antibody. Cells were viewed with an LSM 510 inverted confocal microscope (Carl Zeiss).

Size Exclusion Chromatography. Gel filtration was performed using either Superdex 200 10/300 GL high-resolution resin or Superdex 200 10/300 prep grade resin, equilibrated in 55 mM Tris (pH 8.0), 21 mM NaCl, 0.88 mM KCl, 800 mM guanidine, and arginine (either 800 or 250 mM). Protein samples were first injected onto the gel filtration column individually at a final concentration of 0.75 mg/mL for the p33 protein and 0.4 mg/mL for the p55 protein. To analyze p33/p55 mixtures, the appropriate sizing column fractions corresponding to either p33 or p55 were each concentrated to 1 mg/mL. VacA p33 was added to p55 in a 2:1 volume ratio, the mixture incubated for 45 min at 4 °C, and the p33/p55 mixture then applied to a gel filtration column. Retention volumes of bovine thyroglobulin, alcohol dehydrogenase, bovine serum albumin, and carbonic anhydrase were used as standards to calculate the molecular masses of the purified VacA proteins.

Electron Microscopy. To visualize the morphology of p33/p55 mixtures, appropriate gel filtration fractions containing these proteins were analyzed by electron microscopy (EM) using conventional negative staining as described previously (*55*). Protein solutions were diluted to appropriate final concentrations (25−100 μg/mL), and 2.5 μL aliquots were spotted onto glow-discharged copper-mesh grids (EMS) for approximately 1 min. In some experiments, p33/p55 mixtures were mixed in a 9:1 (v/v) ratio with Brucella broth (*56*) or *n*-dodecyl β-D-maltoside (DDM, Anatrace) prior to EM analysis. The final concentration of DDM was 0.34 mM, which corresponds to twice the critical micelle concentration. The grids were washed in 5 drops of water followed by 1 drop of 0.7% uranyl formate. Grids were then incubated on 1 drop of 0.7% uranyl formate for 1 min, blotted against filter paper, and allowed to air-dry. Initial images of wild-type p88 or the p33/p55 mixture mixed with Brucella broth were collected on an FEI morgagni run at 100 kV at a magnification of 36000×. Images were recorded on an ATM 1Kx1K CCD camera. Images of p88 used for multireference alignment were collected on a FEI 120 kV electron microscope at a magnification of 67000×. Images were recorded on DITABIS (Pforzheim, Germany) digital imaging plates. The plates were scanned on a DITABIS micrometer scanner, converted to mixed raster content (mrc) format, and binned by a factor of 2, yielding final images with 4.48 Å/pixel. Images of the p33/p55 mixture in DDM purified by gel filtration were taken on a 200 kV FEI electron microscope equipped with a field emission electron source and operated at an acceleration voltage of 120 kV and magnification of 100000×. Images were collected using a Gatan 4Kx4K CCD camera. CCD images were converted to mrc format and binned by a factor of 4, resulting in final images with 4.26 Å/pixel. Images of both p88 and the p33/p55 mixture were taken under low-dose conditions using a defocus value of −1.5 μm.

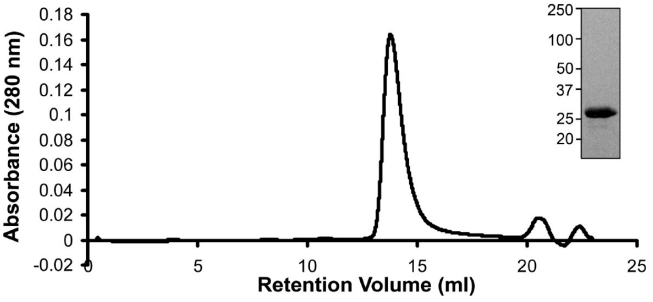

FIGURE 1: Purification of recombinant p33 VacA. SDS−PAGE and Coomassie blue stain of p33 VacA purified under denaturing conditions (inset). Gel filtration chromatography (Superdex 200 10/300 GL high-resolution resin) of p33 VacA after protein refolding, using buffer containing 800 mM guanidine and 800 mM arginine, as described in Experimental Procedures.

For alignment and averaging of p88 VacA and p33/p55 VacA in DDM, 9871 and 1273 images of p88 and p33/p55 VacA particles, respectively, were selected with Boxer and windowed with a 120 pixel side length (*57*). Image analysis was conducted with SPIDER and the associated display program WEB (*58*). The images were rotationally and translationally aligned and subjected to 10 cycles of multireference alignment and K-means classification. For analysis of p88 VacA, alignment particles were first classified into 20 class averages (data not shown) and seven representative classes then were chosen as references for another cycle of multireference alignment. For analysis of p33/p55 VacA, particles were first classified into 10 class averages (data not shown) and then four representative projections were chosen as references for another cycle of multireference alignment.

RESULTS

Expression, Purification, and Refolding of Recombinant p33 VacA. In previous studies, it has not been possible to purify a functionally active form of the p33 domain (*32*). We attempted to purify the p33 VacA fragment from *E. coli* extracts under native conditions but were unsuccessful. Therefore, we expressed and purified the recombinant p33 under denaturing conditions and then used dialysis to reduce the concentration of denaturants and allow the protein to refold. After the p33 protein was refolded, it eluted as a well-defined peak by size exclusion chromatography (Figure 1).

Refolded p33 Mixed with Purified p55 Causes Cellular Alterations. To test the activity of the purified p33 and p55 proteins, we added these proteins individually and in combination to HeLa cells and analyzed the capacity of the proteins to cause cell vacuolation, a hallmark of VacA activity. No detectable vacuolating activity was observed when the p33 or p55 protein was added to cells individually, as demonstrated by the neutral red uptake assay and light microscopic examination of the cells (Figure 2A and data not shown). Similarly, none of the buffers alone or in combination exhibited any detectable activity

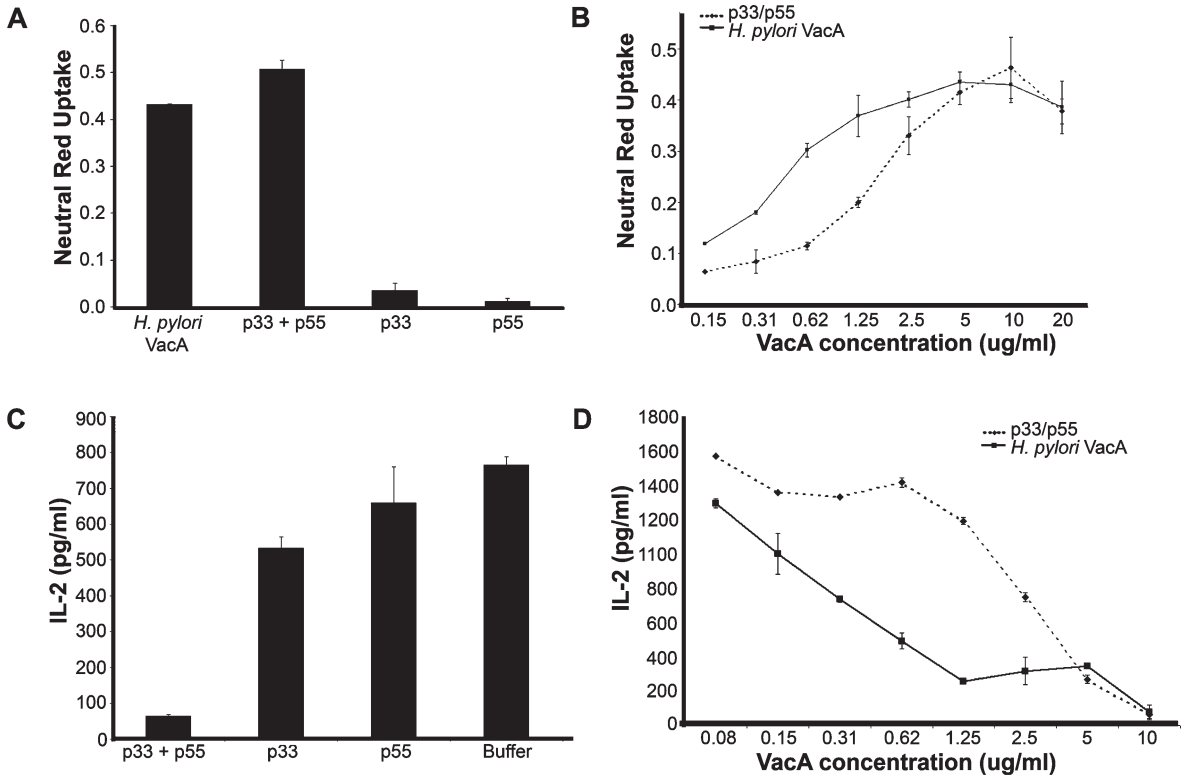

FIGURE 2: Effects of p33 and p55 VacA proteins on HeLa cells and Jurkat cells. Purified refolded p33 and purified p55 (each at 1 mg/mL) were mixed together in a 1:1 mass ratio, which ensured an excess of p33 on a molar basis. The p88 VacA protein purified from the *H. pylori* culture supernatant was acid-activated prior to contact with cells (*42*, *51*), whereas the p33 and p55 preparations were not acid-activated. (A) HeLa cells were incubated with the purified VacA proteins at a final concentration of 10 μg/mL (or 5 μg/mL for each protein in the case of the p33/p55 mixture). Cell vacuolation was quantified by the neutral red uptake assay (OD_{540}). (B) HeLa cells were incubated with the indicated final concentrations of a p33/p55 mixture (20 μg/mL corresponds to 10 μg/mL p33 and 10 μg/mL p55) or the p88 form of VacA purified from the *H. pylori* broth culture supernatant. Cell vacuolation was quantified by the neutral red uptake assay. (C) Jurkat cells were incubated with the indicated purified VacA proteins at a concentration of 6 μg/mL (or 3 μg/mL for each protein in the case of the p33/p55 mixture) for 30 min at 37 °C. The cells were then stimulated, and IL-2 secretion was measured as described in Experimental Procedures. (D) Jurkat cells were incubated with the indicated final concentrations of a p33/p55 mixture or the p88 form of VacA purified from the *H. pylori* culture supernatant. The cells were then stimulated, and IL-2 secretion was measured as described in Experimental Procedures. Results represent the mean ± standard deviation, based on analysis of triplicate samples.

(data not shown). In contrast, a mixture of the purified p33 and p55 proteins caused extensive vacuolation of HeLa cells (Figure 2A,B). The potency of the p33/p55 mixture was slightly lower than that of the p88 VacA protein purified from *H. pylori* broth culture supernatant (Figure 2B). A mixture of p55 and heat-denatured p33 failed to cause any detectable effects on cells (data not shown).

Previous studies have shown that VacA from *H. pylori* inhibits production of IL-2 by Jurkat cells (*21*). To test whether p33 and p55 proteins exhibit a similar activity, we incubated Jurkat cells with the purified p33 and p55 proteins individually and in combination. When added individually, neither p33 nor p55 had any effect on IL-2 secretion (Figure 2C). In contrast, the p33/p55 mixture inhibited IL-2 secretion from Jurkat cells (Figure 2C,D). The potency of the p33/p55 mixture was slightly lower than that of the p88 VacA protein purified from *H. pylori* (Figure 2D). Collectively, these results indicate that the refolded p33 protein, when mixed with the p55 protein, is biologically active and capable of causing alterations in eukaryotic cells.

Refolded p33Δ6−27 Exhibits a Dominant Negative Effect. When certain mutant VacA proteins (e.g., VacAΔ6−27) are mixed with wild-type VacA, the mutant proteins can act as dominant negative inhibitors of wild-type VacA activity (*33*, *47*−*50*). To further validate the new methods for expression and refolding of p33 proteins, we expressed, purified, and refolded the p33Δ6−27 protein under the same conditions used for purification and refolding of the p33 wild-type protein. When added to cells individually or in combination with purified p55, the p33Δ6−27 protein did not cause detectable cell vacuolation (Figure 3A). To test for dominant negative properties of the mutant protein, we premixed the p33Δ6−27 protein with p33/p55 mixtures that were known to be active (Figure 3A). When this p33/p55/p33Δ6−27 mixture was added to cells, no detectable vacuolation was observed, indicating that the mutant protein exhibited a dominant negative effect (Figure 3A). The purified refolded p33Δ6−27 protein, when mixed with purified p55, exhibited dominant negative inhibitory properties similar to those of the p88Δ6−27 protein purified from the *H. pylori* broth culture supernatant (Figure 3B) (*33*, *49*).

Interactions of p33 and p55 with HeLa Cells. Several previous studies have shown that sequences within the p55 domain contribute to the binding of p88 VacA to cells, and it has been suggested that p55 functions as a cell binding domain (*35*−*37*). To investigate the cell binding properties of p55 in further detail, we incubated HeLa cells with purified fluorescently labeled p55. Very little if any interaction of purified p55 with HeLa cells was observed (Figure 4A). In contrast, when p55 was incubated with HeLa cells in the presence of purified refolded p33, a marked increase in the level of binding and uptake of p55 by cells was observed (Figure 4A). Thus, p33 markedly

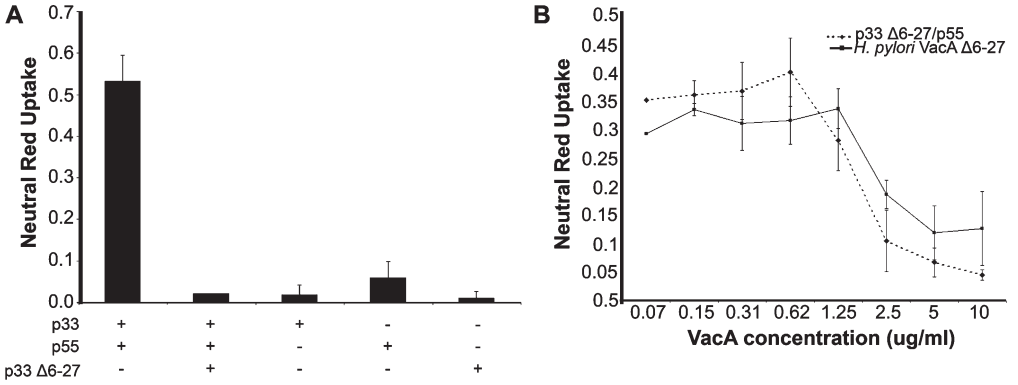

FIGURE 3: Refolded p33Δ6−27 exhibits dominant negative properties. (A) VacA p33Δ6−27 was purified and refolded as described in Experimental Procedures. Purified p33Δ6−27 was mixed with p55 and p33 (each at 1 mg/mL) at a 1:1:1 mass ratio. HeLa cells were then incubated with the indicated recombinant VacA proteins (either individually or in a mixture) at a final concentration of 10 μg/mL for 9 h at 37 °C. Cell vacuolation was quantified by the neutral red uptake assay. (B) Wild-type p88 VacA (5 μg/mL) was incubated with the indicated concentrations of the VacA p33Δ6−27/p55 mixture or the p88Δ6−27 VacA protein purified from the *H. pylori* culture supernatant. Cell vacuolation was quantified by the neutral red uptake assay. Results represent the mean ± standard deviation, based on analysis of triplicate samples.

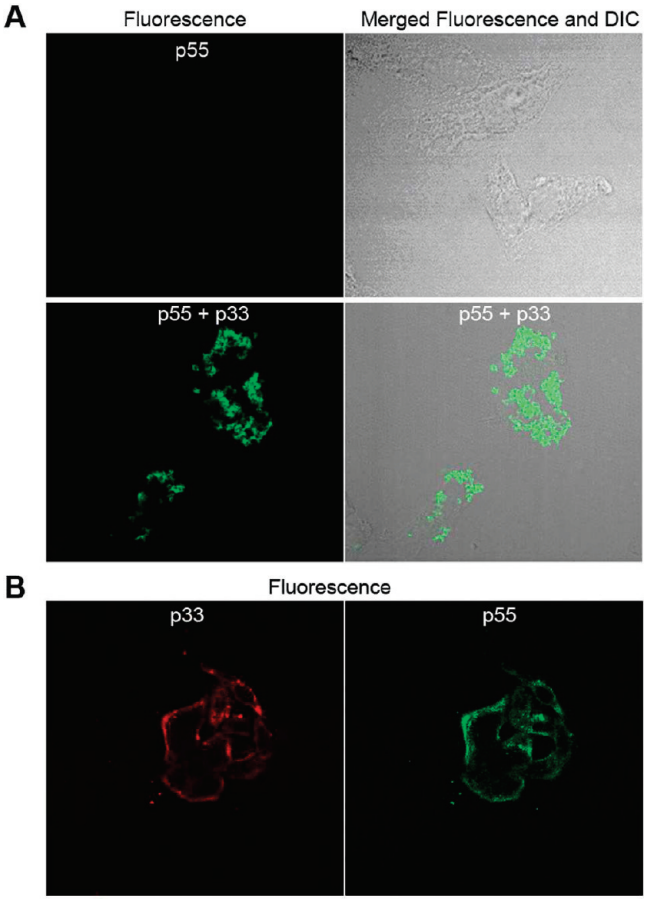

FIGURE 4: Interaction of p55 and p33 proteins with HeLa cells. (A) HeLa cells were incubated with Alexa 488-labeled p55 alone (10 μg/mL) or a mixture of labeled p55 and purified refolded p33 (5 μg/mL each) for 4 h at 37 °C. Cells were imaged as described in Experimental Procedures. (B) Cells were incubated with purified Alexa 488-labeled p55 and purified refolded c-Myc-tagged p33 protein for 1 h at 37 °C. The c-Myc-tagged p33 protein was detected by indirect immunofluorescence.

enhanced the cell binding properties of p55. Further studies indicated that when a mixture of p33 and p55 was incubated with cells, both p33 and p55 bound to the cell surface (Figure 4B). These properties of purified p33 and p55 proteins are consistent with previously observed properties of p33 and p55 proteins contained in crude *E. coli* extracts (*32*).

Interaction of Refolded p33 with Purified p55. To investigate potential interactions among the purified p33 and p55 proteins, we performed size exclusion chromatography experiments. When the refolded wild-type p33 protein was analyzed, a peak with a predicted mass of ~96 kDa was observed (Figure 5, red peak with an asterisk). When the purified p55 protein was analyzed, a peak with a molecular mass of 178 kDa was observed (Figure 5, green peak with an asterisk). When the p33/p55 mixture was analyzed, a peak with a predicted mass of 86 kDa was observed (Figure 5, blue peak with an asterisk), the 96 kDa peak (corresponding to p33 alone) was lost, and the 178 kDa peak (corresponding to p55 alone) was minimized. Representative fractions were tested by SDS−PAGE and Coomassie blue staining; this revealed an approximate 33 kDa band for the VacA 96 kDa peak, a 55 kDa band for the 178 kDa peak, and two protein bands of 33 and 55 kDa for the 86 kDa peak (Figure 5B). When tested in cell culture assays, the p33/p55 mixture corresponding to the blue peak in Figure 5 caused cell vacuolation with a potency similar to that shown in Figure 2B (data not shown). Taken together, these results suggest that the refolded p33 protein interacts with the purified p55 protein to yield a p33/p55 complex. Moreover, these data suggest that p33 homo-oligomers and p55 homo-oligomers must undergo disassembly to interact with each other and form 88 kDa p33/p55 complexes.

Assembly of p33/p55 Complexes into Oligomeric Structures. The p88 VacA protein secreted by *H. pylori* can assemble into water-soluble oligomers (*42*−*45*). To investigate the possibility that p33 and p55 domains might assemble into similar structures, we visualized the p33/p55 mixture (purified by gel filtration as a monomeric complex) by EM. VacA p88 oligomers purified from the *H. pylori* culture supernatant (and exchanged into guanidine- and arginine-containing buffer by gel filtration) were analyzed as a control. As expected, large flowerlike structures were visualized in preparations of *H. pylori* p88 VacA (Figure 6A). In contrast, the p33/p55 mixture consisted mainly of small rodlike particles (Figure 6B), similar to the appearance of p88 monomers produced by *H. pylori* (*42*, *43*).

To explain why p88 proteins in the *H. pylori* broth culture supernatant readily assemble into flowerlike oligomeric structures whereas purified p33 and p55 proteins do not, we hypothesized that the broth culture medium used for growth of *H. pylori* (a nutrient-rich medium prepared from yeast extract and animal

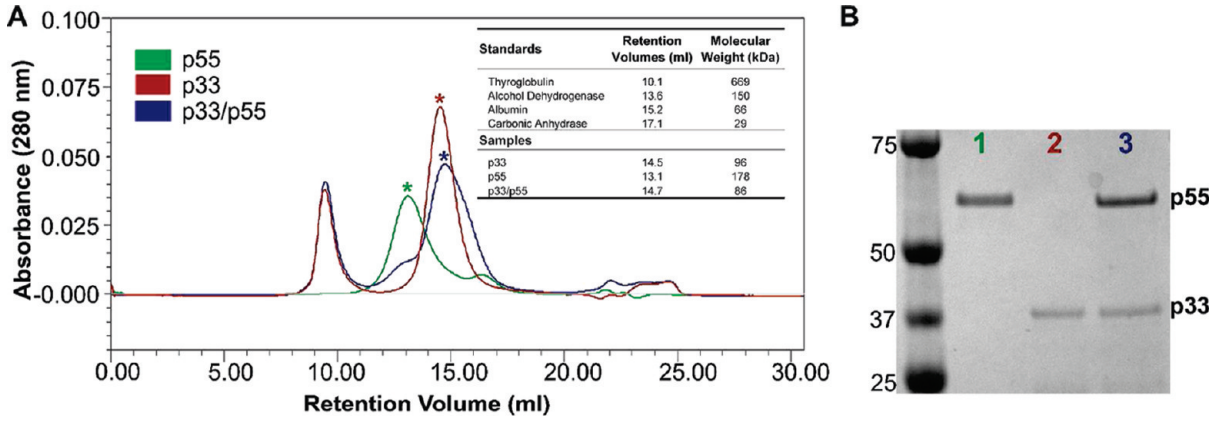

FIGURE 5: Analysis of p33 and p55 proteins by gel filtration. (A) Size exclusion chromatography (Superdex 200 10/300 prep grade resin) of refolded p33 (red peak), purified p55 (green peak), or a mixture of the two proteins (blue peak). Refolded p33 and purified p55 (each 1 mg/mL) were mixed at a 2:1 mass ratio and injected into the sizing column, as described in Experimental Procedures. The buffer contained 800 mM guanidine and 250 mM arginine, which were required to maintain the solubility of the p33 protein. The inset shows retention volumes of p33, p55, and the p33/p55 mixture in comparison to those of standard proteins. (B) The lower-molecular mass peaks (asterisks) from each of the size exclusion chromatography experiments shown in panel A were analyzed by SDS−PAGE and Coomassie blue staining.

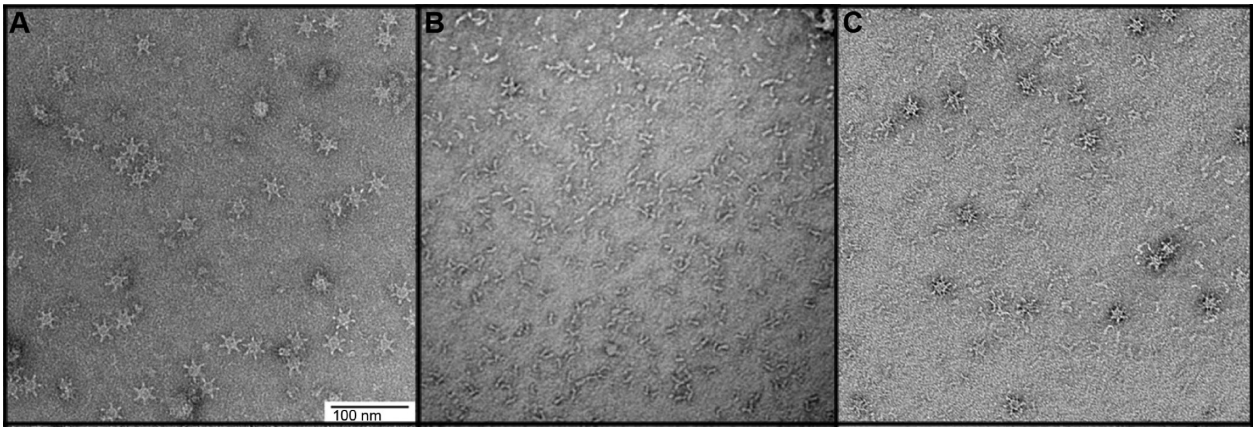

FIGURE 6: Assembly of p33 and p55 proteins into oligomeric structures. EM analysis of (A) p88 purified from the *H. pylori* culture supernatant and then exchanged into a guanidine-containing buffer by gel filtration or (B) a mixture of refolded p33 and p55 that eluted from the sizing column (corresponding to Figure 5A, blue peak with an asterisk). (C) The p33/p55 preparation shown in panel B was mixed with Brucella broth as described in Experimental Procedures and then analyzed by EM. The images in this figure represent analysis of at least three grids for each condition and analysis of > 10 fields per grid. The scale bar is 100 nm for all panels.

tissue, known as Brucella broth) might contain factors that promote VacA oligomerization. To test this hypothesis, we examined the appearance of the p33/p55 mixture by EM, either in the presence or in the absence of added Brucella broth. In the presence of added Brucella broth, an increased level of formation of flower-shaped complexes was detected (Figure 6C). These experiments indicated that Brucella broth stimulates the oligomerization of p33/p55 mixtures into oligomeric structures similar to those formed by p88 VacA from *H. pylori*.

High-Resolution Imaging of p33/p55 Oligomeric Complexes. We reasoned that the complex mixture of components in Brucella broth, including numerous membrane-derived factors, promoted the formation of flowerlike oligomers. In an effort to stimulate VacA oligomerization using more refined conditions, we incubated p33/p55 mixtures with various additives designed to create an amphipathic environment, including bovine heart total extract solubilized in chloroform, chloroform alone, and the detergent dodecyl β-D-maltoside (DDM). Each of these additives promoted oligomerization of the p33/p55 monomeric complexes into flowerlike oligomeric structures (data not shown). The VacA oligomers formed in the presence of bovine heart extract or chloroform had a more heterogeneous appearance than the VacA oligomers formed in the presence of DDM, and therefore, we studied the latter oligomers in further detail. To permit higher-resolution imaging, p33/p55 monomeric complexes (corresponding to the 86 kDa blue peak in Figure 5) were mixed with DDM, dialyzed, and passed over a gel filtration column in the presence of DDM and arginine and the absence of guanidine. Under these conditions, the 86 kDa peak was minimized and a high-molecular mass (> 300 kDa) peak was observed (data not shown). High-molecular mass complexes containing wild-type p33 and p55 were isolated and analyzed further by EM. The appearance of these oligomers (Figure 7A) was similar to that of p88 oligomers isolated from *H. pylori* broth culture supernatant (Figure 7B). To further characterize the structural features of p33/p55 oligomers, approximately 1300 particles were classified into 10 groups and four classes were chosen as references for an additional round of reference based-alignment (Figure 7C and data not shown). To directly compare the structural organization of p33/p55 oligomers with that of p88 oligomers purified from *H. pylori* broth culture supernatant, class averages of p88 oligomers were also generated. Because p88 oligomers seemed to adopt a larger number of conformations than p33/p55 oligomers, a larger number of p88 images were classified. Approximately 10000

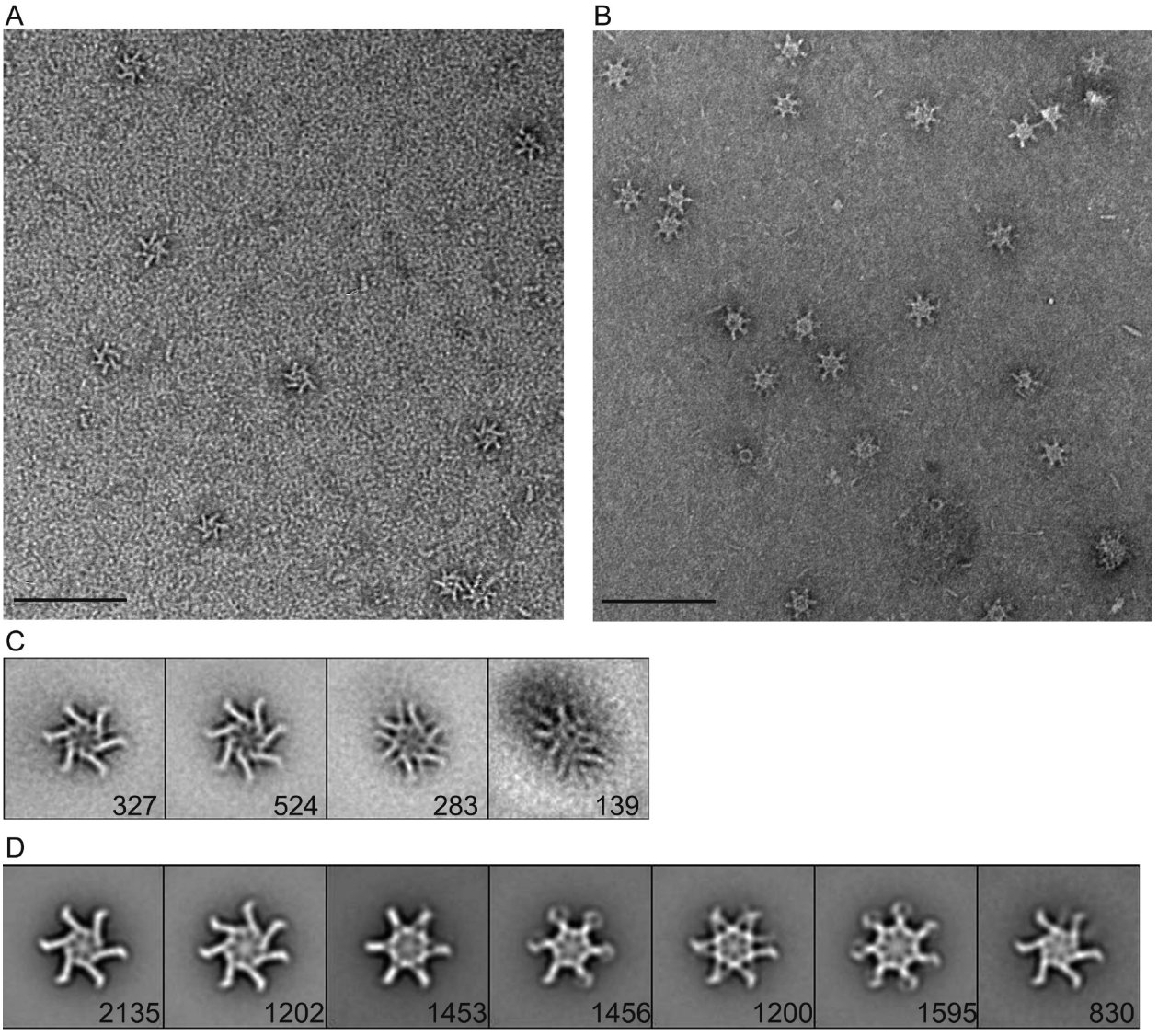

FIGURE 7: Analysis of p33/p55 VacA oligomers in negative stain. Mixtures of refolded p33 and p55 eluted from the sizing column (corresponding to Figure 5A, blue peak with an asterisk) were mixed with DDM and then dialyzed overnight in buffer containing 55 mM Tris (pH 8.0), 21 mM NaCl, 0.88 mM KCl, 250 mM arginine, and DDM. The protein was passed over a gel filtration column that was equilibrated with dialysis buffer containing DDM, and VacA oligomers eluting in a high-molecular mass fraction were then analyzed by EM. (A) Representative image of negatively stained p33/p55 VacA oligomers eluting in a high-molecular mass fraction. The scale bar is 100 nm. (B) Representative image of negatively stained p88 VacA oligomers isolated from *H. pylori* broth culture supernatant. The scale bar is 100 nm. (C) Four class averages of p33/p55 VacA particles in negative stain generated from reference-based alignment. The number of particles in each projection average is shown in the bottom right corner of each average. The side length of individual panels is 511 Å. (D) Seven representative class averages of p88 VacA particles in negative stain generated from reference-based alignment. The number of particles in each projection average is shown in the bottom right corner of each average. The side length of individual panels is 538 Å.

particles of p88 VacA were classified into 20 class averages (data not shown), and seven classes were chosen for an additional round of reference-based alignment (Figure 7D and data not shown).

The result of the p33/p55 complex alignment (Figure 7C) shows that the majority of the p33/p55 oligomers are composed of six or seven subunits [67% (Figure 7C, panels 1 and 2)], with one smaller class composed of an oligomer with 12 visible subunits [22% (Figure 7C, panel 3)] and one class representing poorly formed oligomers (Figure 7C, panel 4). The 12-subunit complex may represent a double-layer oligomer with the two layers splayed (*43*, *44*). The overall appearances of hexameric and heptameric p33/p55 oligomers are reminiscent of single-layer hexameric and heptameric oligomers formed by p88 VacA (Figure 7D, panels 1 and 2) (*42*−*44*). These single-layer oligomers exhibit a striking chirality, which suggests that one surface adsorbs preferentially to the support film. In contrast to the p33/p55 oligomers, a majority of the p88 oligomers exist as double-layer complexes containing 12−14 subunits (Figure 7D, panels 3−6) (*42*−*44*). Importantly, difference maps created between averages of p33/p55 and p88 single-layer heptameric and hexameric oligomers did not show any statistically relevant difference peaks (data not shown), which indicates that these oligomeric forms are structurally equivalent.

DISCUSSION

In this study, we demonstrate that a functionally active form of *H. pylori* VacA can be reconstituted from two purified VacA fragments (p33 and p55). Previously, the p55 fragment was purified and its crystal structure determined (*39*), but it was not possible to purify a soluble, functionally active form of p33.

In this study, we purified the p33 domain under denaturing conditions and then employed a series of steps designed to allow the protein to refold and remain soluble. We found that the refolded p33 protein was soluble in a buffer containing 800 mM guanidine and 250 mM arginine, but upon removal of these additives, the p33 protein became insoluble. Analysis of the p33 protein by circular dichroism was not feasible because of interference caused by the presence of arginine. Nevertheless, in comparison to denatured p33, the refolded p33 protein exhibited functional activity when mixed with the p55 fragment, which suggests that the p33 protein was successfully refolded.

Previous studies reported that a mixture of *E. coli* lysates containing VacA p33 and p55 can cause vacuolation of HeLa cells (*32*), and intracellular coexpression of p33 and p55 in HeLa cells results in cell vacuolation (*38*, *59*). However, there are numerous limitations associated with the use of crude *E. coli* lysates or intracellular expression systems. By using purified p33 and p55 proteins in this study, we were able to monitor the process by which p33 and p55 proteins interact to yield a functionally active VacA protein. Specifically, we demonstrate that the p33 and p55 proteins were purified with molecular masses of ~96 and ~178 kDa, respectively. The mass of the p33 protein is consistent with a trimeric form, but efforts to validate this by EM were unsuccessful. The mass of the p55 protein is consistent with a trimer as well, but the crystal structure of p55 revealed a head-to-head packed dimer that adopts an elongated dumbbell shape (*39*). The elongated shape and the unusual buffer conditions likely account for the high apparent molecular mass of p55 on the sizing column. When the p55 and p33 preparations are mixed, the p55 and p33 homo-oligomers each dissociated to yield a p33/p55 complex with a mass of ~86 kDa, corresponding to a complex containing one p55 subunit and one p33 subunit. These p33/p55 monomeric complexes were visible by EM as elongated rods (Figure 6), similar to the appearance of p88 VacA monomers (*43*).

The ability to reconstitute a functional protein from two individually expressed component domains is somewhat unusual among bacterial protein toxins, and unusual among proteins in general. This phenomenon is probably facilitated by distinctive structural features of VacA. The VacA p55 domain consists predominantly of a β-helix, composed of multiple ~25-amino acid repeats, each of which forms a three-β-strand triangle-shaped coil (*39*). Adjacent coils are held together by backbone hydrogen bonds. The β-helix is therefore very different from globular proteins where adjacent structural elements are held together with an intricate arrangement of side chain interactions. On the basis of computer modeling, the VacA p33 domain is also predicted to comprise a β-helical structure, and it is predicted that the p88 protein comprises an elongated continuous β-helical structure (*39*). In the experiments described here, we speculate that the C-terminal coil of p33 interacts with the N-terminal coil of p55, recapitulating the structural relationship that exists between these two domains in the intact p88 VacA protein (*39*).

A distinctive property of the p88 VacA protein secreted by *H. pylori* is its ability to assemble into water-soluble, flower-shaped oligomeric structures (*42*−*45*). In contrast, we observed that purified p33 and p55 proteins interact to form ~86 kDa complexes but do not readily assemble into oligomeric structures when maintained in buffer alone. One possible explanation is that the guanidine and arginine constituents of the buffer (required for maintenance of p33 solubility) prevent VacA oligomerization; however, we observed that these agents did not cause disassembly of p88 oligomers purified from the *H. pylori* culture supernatant. We hypothesized that the *H. pylori* broth culture supernatant might contain factors (either components of the rich Brucella broth medium used for culture of *H. pylori* or additional *H. pylori* products) that allow VacA oligomers to form. We observed that, indeed, the addition of freshly prepared Brucella broth (not previously cultured with *H. pylori*) to purified p33/p55 mixtures promoted assembly of VacA into oligomeric structures. Similarly, the addition of detergent also stimulated oligomerization. We speculate that oligomerization is stimulated by exposure to an amphipathic environment and that the oligomerization observed in these experiments mimics the process by which VacA oligomerizes when in contact with membranes of host cells.

The p88 VacA protein is typically purified in an oligomeric form from the *H. pylori* broth culture supernatant (*8*, *42*−*45*), and monomeric forms of p88 VacA have been relatively difficult to purify. When added to cultured eukaryotic cells, purified p88 VacA oligomers lack detectable activity in most assays unless the oligomers are first exposed to low-pH or high-pH conditions, which results in oligomer disassembly; oligomers have been observed to reassemble if the pH is returned to neutral (*16*, *24*, *42*, *51*, *60*−*62*). A current model presumes that VacA monomers interact with the cell surface and then reassemble into oligomeric complexes that function as membrane channels. In our study, we demonstrate that a mixture of purified p33 and p55 proteins is fully active in cell culture assays in the absence of low-pH or high-pH activation. Since the p33/p55 mixture predominantly consists of a p88 complex (Figures 5 and 6), this provides additional support for a model in which VacA monomers interact with the plasma membrane.

Several lines of evidence indicate that oligomerization of p88 VacA is required for VacA-induced cellular alterations (*33*, *47*, *48*, *50*). VacA oligomeric structures have been visualized on the surface of VacA-treated cells or lipid bilayers (*24*, *44*, *46*), and in contrast to double-layer oligomeric forms of VacA found in *H. pylori* culture supernatant, there is evidence that the VacA oligomeric complexes formed on the surface of cells are single-layer (*24*). Potentially, oligomerization of VacA occurs preferentially within lipid raft components of the plasma membrane (*46*, *63*, *64*). In this study, we observed that detergent promoted assembly of p33/p55 mixtures into predominantly single-layer oligomeric structures. Therefore, the complexes visualized in this study are predicted to be useful models for VacA channels that form in the context of human cells.

The reconstitution of VacA activity from purified p33 and p55 components probably involves a complex series of molecular events. An initial step involves disassembly of p33 and p55 homo-oligomers and formation of a p33/p55 complex. Potentially, the presence of p55 disrupts p33/p33 interactions, or the presence of p33 may disrupt p55/p55 interactions. An important observation is that neither p33 nor p55 bound to cells when added individually, whereas the p33/p55 mixture exhibited strong binding to cells (Figure 4). One possible explanation is that the homo-oligomeric forms of p33 and p55 lack cell binding activity, and cell binding surfaces become exposed upon disassembly of the homo-oligomeric complexes. Alternatively, the receptor binding site(s) may span both the p33 and p55 domains. Finally, the assembly of p33/p55 complexes into higher-order flower-shaped oligomers may stabilize the interaction of VacA with the surface of eukaryotic cells, and oligomer formation is predicted to be required for insertion of VacA into membranes and channel formation.

ACKNOWLEDGMENT

We thank D. Williams and B. Hosse for EM and microbiology technical support, respectively. We thank J. D. King and J. F. Hillyer for advice on microscopic techniques. Cell imaging experiments were performed through the use of the VUMC Cell Imaging Shared Resource (supported by National Institutes of Health Grants CA68485, DK20593, DK58404, HD15052, DK59637, and EY08126).

REFERENCES

1. Marshall, B. J., and Warren, J. R. (1984) Unidentified curved bacilli in the stomach of patients with gastritis and peptic ulceration. *Lancet 1*, 1311–1315.
2. Dunn, B. E., Cohen, H., and Blaser, M. J. (1997) *Helicobacter pylori*. *Clin. Microbiol. Rev. 10*, 720–741.
3. Cover, T. L., and Blaser, M. J. (2009) *Helicobacter pylori* in health and disease. *Gastroenterology 136*, 1863–1873.
4. Atherton, J. C., and Blaser, M. J. (2009) Coadaptation of *Helicobacter pylori* and humans: Ancient history, modern implications. *J. Clin. Invest. 119*, 2475–2487.
5. Amieva, M. R., and El-Omar, E. M. (2008) Host-bacterial interactions in *Helicobacter pylori* infection. *Gastroenterology 134*, 306–323.
6. Atherton, J. C. (2006) The pathogenesis of *Helicobacter pylori*-induced gastro-duodenal diseases. *Annu. Rev. Pathol. 1*, 63–96.
7. Leunk, R. D., Johnson, P. T., David, B. C., Kraft, W. G., and Morgan, D. R. (1988) Cytotoxic activity in broth-culture filtrates of *Campylobacter pylori*. *J. Med. Microbiol. 26*, 93–99.
8. Cover, T. L., and Blaser, M. J. (1992) Purification and characterization of the vacuolating toxin from *Helicobacter pylori*. *J. Biol. Chem. 267*, 10570–10575.
9. Cover, T. L., and Blanke, S. R. (2005) *Helicobacter pylori* VacA, a paradigm for toxin multifunctionality. *Nat. Rev. Microbiol. 3*, 320–332.
10. de Bernard, M., Cappon, A., Del Giudice, G., Rappuoli, R., and Montecucco, C. (2004) The multiple cellular activities of the VacA cytotoxin of *Helicobacter pylori*. *Int. J. Med. Microbiol. 293*, 589–597.
11. Fischer, W., Prassl, S., and Haas, R. (2009) Virulence mechanisms and persistence strategies of the human gastric pathogen *Helicobacter pylori*. *Curr. Top. Microbiol. Immunol. 337*, 129–171.
12. Fujikawa, A., Shirasaka, D., Yamamoto, S., Ota, H., Yahiro, K., Fukada, M., Shintani, T., Wada, A., Aoyama, N., Hirayama, T., Fukamachi, H., and Noda, M. (2003) Mice deficient in protein tyrosine phosphatase receptor type Z are resistant to gastric ulcer induction by VacA of *Helicobacter pylori*. *Nat. Genet. 33*, 375–381.
13. Telford, J. L., Ghiara, P., Dell'Orco, M., Comanducci, M., Burroni, D., Bugnoli, M., Tecce, M. F., Censini, S., Covacci, A., and Xiang, Z.; et al. (1994) Gene structure of the *Helicobacter pylori* cytotoxin and evidence of its key role in gastric disease. *J. Exp. Med. 179*, 1653–1658.
14. Atherton, J. C., Cao, P., Peek, R. M., Jr., Tummuru, M. K., Blaser, M. J., and Cover, T. L. (1995) Mosaicism in vacuolating cytotoxin alleles of *Helicobacter pylori*. Association of specific *vacA* types with cytotoxin production and peptic ulceration. *J. Biol. Chem. 270*, 17771–17777.
15. Figueiredo, C., Machado, J. C., Pharoah, P., Seruca, R., Sousa, S., Carvalho, R., Capelinha, A. F., Quint, W., Caldas, C., van Doorn, L. J., Carneiro, F., and Sobrinho-Simoes, M. (2002) *Helicobacter pylori* and interleukin 1 genotyping: An opportunity to identify high-risk individuals for gastric carcinoma. *J. Natl. Cancer Inst. 94*, 1680–1687.
16. Szabo, I., Brutsche, S., Tombola, F., Moschioni, M., Satin, B., Telford, J. L., Rappuoli, R., Montecucco, C., Papini, E., and Zoratti, M. (1999) Formation of anion-selective channels in the cell plasma membrane by the toxin VacA of *Helicobacter pylori* is required for its biological activity. *EMBO J. 18*, 5517–5527.
17. Galmiche, A., Rassow, J., Doye, A., Cagnol, S., Chambard, J. C., Contamin, S., de Thillot, V., Just, I., Ricci, V., Solcia, E., Van Obberghen, E., and Boquet, P. (2000) The N-terminal 34 kDa fragment of *Helicobacter pylori* vacuolating cytotoxin targets mitochondria and induces cytochrome c release. *EMBO J. 19*, 6361–6370.
18. Willhite, D. C., and Blanke, S. R. (2004) *Helicobacter pylori* vacuolating cytotoxin enters cells, localizes to the mitochondria, and induces mitochondrial membrane permeability changes correlated to toxin channel activity. *Cell. Microbiol. 6*, 143–154.
19. Nakayama, M., Kimura, M., Wada, A., Yahiro, K., Ogushi, K., Niidome, T., Fujikawa, A., Shirasaka, D., Aoyama, N., Kurazono, H., Noda, M., Moss, J., and Hirayama, T. (2004) *Helicobacter pylori* VacA activates the p38/activating transcription factor 2-mediated signal pathway in AZ-521 cells. *J. Biol. Chem. 279*, 7024–7028.
20. Terebiznik, M. R., Raju, D., Vazquez, C. L., Torbricki, K., Kulkarni, R., Blanke, S. R., Yoshimori, T., Colombo, M. I., and Jones, N. L. (2009) Effect of *Helicobacter pylori*'s vacuolating cytotoxin on the autophagy pathway in gastric epithelial cells. *Autophagy 5*, 370–379.
21. Gebert, B., Fischer, W., Weiss, E., Hoffmann, R., and Haas, R. (2003) *Helicobacter pylori* vacuolating cytotoxin inhibits T lymphocyte activation. *Science 301*, 1099–1102.
22. Sundrud, M. S., Torres, V. J., Unutmaz, D., and Cover, T. L. (2004) Inhibition of primary human T cell proliferation by *Helicobacter pylori* vacuolating toxin (VacA) is independent of VacA effects on IL-2 secretion. *Proc. Natl. Acad. Sci. U.S.A. 101*, 7727–7732.
23. Sewald, X., Gebert-Vogl, B., Prassl, S., Barwig, I., Weiss, E., Fabbri, M., Osicka, R., Schiemann, M., Busch, D. H., Semmrich, M., Holzmann, B., Sebo, P., and Haas, R. (2008) Integrin subunit CD18 Is the T-lymphocyte receptor for the *Helicobacter pylori* vacuolating cytotoxin. *Cell Host Microbe 3*, 20–29.
24. Czajkowsky, D. M., Iwamoto, H., Cover, T. L., and Shao, Z. (1999) The vacuolating toxin from *Helicobacter pylori* forms hexameric pores in lipid bilayers at low pH. *Proc. Natl. Acad. Sci. U.S.A. 96*, 2001–2006.
25. Tombola, F., Carlesso, C., Szabo, I., de Bernard, M., Reyrat, J. M., Telford, J. L., Rappuoli, R., Montecucco, C., Papini, E., and Zoratti, M. (1999) *Helicobacter pylori* vacuolating toxin forms anion-selective channels in planar lipid bilayers: Possible implications for the mechanism of cellular vacuolation. *Biophys. J. 76*, 1401–1409.
26. Gauthier, N. C., Monzo, P., Gonzalez, T., Doye, A., Oldani, A., Gounon, P., Ricci, V., Cormont, M., and Boquet, P. (2007) Early endosomes associated with dynamic F-actin structures are required for late trafficking of *H. pylori* VacA toxin. *J. Cell Biol. 177*, 343–354.
27. Cover, T. L., Tummuru, M. K., Cao, P., Thompson, S. A., and Blaser, M. J. (1994) Divergence of genetic sequences for the vacuolating cytotoxin among *Helicobacter pylori* strains. *J. Biol. Chem. 269*, 10566–10573.
28. Schmitt, W., and Haas, R. (1994) Genetic analysis of the *Helicobacter pylori* vacuolating cytotoxin: Structural similarities with the IgA protease type of exported protein. *Mol. Microbiol. 12*, 307–319.
29. Fischer, W., Buhrdorf, R., Gerland, E., and Haas, R. (2001) Outer membrane targeting of passenger proteins by the vacuolating cytotoxin autotransporter of *Helicobacter pylori*. *Infect. Immun. 69*, 6769–6775.
30. Nguyen, V. Q., Caprioli, R. M., and Cover, T. L. (2001) Carboxy-terminal proteolytic processing of *Helicobacter pylori* vacuolating toxin. *Infect. Immun. 69*, 543–546.
31. Torres, V. J., McClain, M. S., and Cover, T. L. (2004) Interactions between p-33 and p-55 domains of the *Helicobacter pylori* vacuolating cytotoxin (VacA). *J. Biol. Chem. 279*, 2324–2331.
32. Torres, V. J., Ivie, S. E., McClain, M. S., and Cover, T. L. (2005) Functional properties of the p33 and p55 domains of the *Helicobacter pylori* vacuolating cytotoxin. *J. Biol. Chem. 280*, 21107–21114.
33. Vinion-Dubiel, A. D., McClain, M. S., Czajkowsky, D. M., Iwamoto, H., Ye, D., Cao, P., Schraw, W., Szabo, G., Blanke, S. R., Shao, Z., and Cover, T. L. (1999) A dominant negative mutant of *Helicobacter pylori* vacuolating toxin (VacA) inhibits VacA-induced cell vacuolation. *J. Biol. Chem. 274*, 37736–37742.
34. McClain, M. S., Iwamoto, H., Cao, P., Vinion-Dubiel, A. D., Li, Y., Szabo, G., Shao, Z., and Cover, T. L. (2003) Essential role of a GXXXG motif for membrane channel formation by *Helicobacter pylori* vacuolating toxin. *J. Biol. Chem. 278*, 12101–12108.
35. Pagliaccia, C., de Bernard, M., Lupetti, P., Ji, X., Burroni, D., Cover, T. L., Papini, E., Rappuoli, R., Telford, J. L., and Reyrat, J. M. (1998) The m2 form of the *Helicobacter pylori* cytotoxin has cell type-specific vacuolating activity. *Proc. Natl. Acad. Sci. U.S.A. 95*, 10212–10217.
36. Reyrat, J. M., Lanzavecchia, S., Lupetti, P., de Bernard, M., Pagliaccia, C., Pelicic, V., Charrel, M., Ulivieri, C., Norais, N., Ji, X., Cabiaux, V., Papini, E., Rappuoli, R., and Telford, J. L. (1999) 3D imaging of the 58 kDa cell binding subunit of the *Helicobacter pylori* cytotoxin. *J. Mol. Biol. 290*, 459–470.
37. Wang, H. J., and Wang, W. C. (2000) Expression and binding analysis of GST-VacA fusions reveals that the C-terminal approximately 100-residue segment of exotoxin is crucial for binding in HeLa cells. *Biochem. Biophys. Res. Commun. 278*, 449–454.
38. Ye, D., Willhite, D. C., and Blanke, S. R. (1999) Identification of the minimal intracellular vacuolating domain of the *Helicobacter pylori* vacuolating toxin. *J. Biol. Chem. 274*, 9277–9282.
39. Gangwer, K. A., Mushrush, D. J., Stauff, D. L., Spiller, B., McClain, M. S., Cover, T. L., and Lacy, D. B. (2007) Crystal structure of the *Helicobacter pylori* vacuolating toxin p55 domain. *Proc. Natl. Acad. Sci. U.S.A. 104*, 16293–16298.

40. Dautin, N., and Bernstein, H. D. (2007) Protein secretion in gram-negative bacteria via the autotransporter pathway. *Annu. Rev. Microbiol. 61*, 89–112.
41. Junker, M., Schuster, C. C., McDonnell, A. V., Sorg, K. A., Finn, M. C., Berger, B., and Clark, P. L. (2006) Pertactin β-helix folding mechanism suggests common themes for the secretion and folding of autotransporter proteins. *Proc. Natl. Acad. Sci. U.S.A. 103*, 4918–4923.
42. Cover, T. L., Hanson, P. I., and Heuser, J. E. (1997) Acid-induced dissociation of VacA, the *Helicobacter pylori* vacuolating cytotoxin, reveals its pattern of assembly. *J. Cell Biol. 138*, 759–769.
43. El-Bez, C., Adrian, M., Dubochet, J., and Cover, T. L. (2005) High resolution structural analysis of *Helicobacter pylori* VacA toxin oligomers by cryo-negative staining electron microscopy. *J. Struct. Biol. 151*, 215–228.
44. Adrian, M., Cover, T. L., Dubochet, J., and Heuser, J. E. (2002) Multiple oligomeric states of the *Helicobacter pylori* vacuolating toxin demonstrated by cryo-electron microscopy. *J. Mol. Biol. 318*, 121–133.
45. Lupetti, P., Heuser, J. E., Manetti, R., Massari, P., Lanzavecchia, S., Bellon, P. L., Dallai, R., Rappuoli, R., and Telford, J. L. (1996) Oligomeric and subunit structure of the *Helicobacter pylori* vacuolating cytotoxin. *J. Cell Biol. 133*, 801–807.
46. Geisse, N. A., Cover, T. L., Henderson, R. M., and Edwardson, J. M. (2004) Targeting of *Helicobacter pylori* vacuolating toxin to lipid raft membrane domains analysed by atomic force microscopy. *Biochem. J. 381*, 911–917.
47. Ivie, S. E., McClain, M. S., Torres, V. J., Algood, H. M., Lacy, D. B., Yang, R., Blanke, S. R., and Cover, T. L. (2008) *Helicobacter pylori* VacA subdomain required for intracellular toxin activity and assembly of functional oligomeric complexes. *Infect. Immun. 76*, 2843–2851.
48. Genisset, C., Galeotti, C. L., Lupetti, P., Mercati, D., Skibinski, D. A., Barone, S., Battistutta, R., de Bernard, M., and Telford, J. L. (2006) A *Helicobacter pylori* vacuolating toxin mutant that fails to oligomerize has a dominant negative phenotype. *Infect. Immun. 74*, 1786–1794.
49. Torres, V. J., McClain, M. S., and Cover, T. L. (2006) Mapping of a domain required for protein-protein interactions and inhibitory activity of a *Helicobacter pylori* dominant-negative VacA mutant protein. *Infect. Immun. 74*, 2093–2101.
50. McClain, M. S., Cao, P., Iwamoto, H., Vinion-Dubiel, A. D., Szabo, G., Shao, Z., and Cover, T. L. (2001) A 12-amino-acid segment, present in type s2 but not type s1 *Helicobacter pylori* VacA proteins, abolishes cytotoxin activity and alters membrane channel formation. *J. Bacteriol. 183*, 6499–6508.
51. de Bernard, M., Papini, E., de Filippis, V., Gottardi, E., Telford, J., Manetti, R., Fontana, A., Rappuoli, R., and Montecucco, C. (1995) Low pH activates the vacuolating toxin of *Helicobacter pylori*, which becomes acid and pepsin resistant. *J. Biol. Chem. 270*, 23937–23940.
52. Middelberg, A. P. (2002) Preparative protein refolding. *Trends Biotechnol. 20*, 437–443.
53. Cover, T. L., Puryear, W., Perez-Perez, G. I., and Blaser, M. J. (1991) Effect of urease on HeLa cell vacuolation induced by *Helicobacter pylori* cytotoxin. *Infect. Immun. 59*, 1264–1270.
54. Algood, H. M., Torres, V. J., Unutmaz, D., and Cover, T. L. (2007) Resistance of primary murine CD4+ T cells to *Helicobacter pylori* vacuolating cytotoxin. *Infect. Immun. 75*, 334–341.
55. Ohi, M., Li, Y., Cheng, Y., and Walz, T. (2004) Negative Staining and Image Classification: Powerful Tools in Modern Electron Microscopy. *Biol. Proced. Online 6*, 23–34.
56. Hawrylik, S. J., Wasilko, D. J., Haskell, S. L., Gootz, T. D., and Lee, S. E. (1994) Bisulfite or sulfite inhibits growth of *Helicobacter pylori*. *J. Clin. Microbiol. 32*, 790–792.
57. Ludtke, S. J., Baldwin, P. R., and Chiu, W. (1999) EMAN: Semi-automated software for high-resolution single-particle reconstructions. *J. Struct. Biol. 128*, 82–97.
58. Frank, J., Radermacher, M., Penczek, P., Zhu, J., Li, Y., Ladjadj, M., and Leith, A. (1996) SPIDER and WEB: Processing and visualization of images in 3D electron microscopy and related fields. *J. Struct. Biol. 116*, 190–199.
59. Ye, D., and Blanke, S. R. (2002) Functional complementation reveals the importance of intermolecular monomer interactions for *Helicobacter pylori* VacA vacuolating activity. *Mol. Microbiol. 43*, 1243–1253.
60. Tombola, F., Oregna, F., Brutsche, S., Szabo, I., Del Giudice, G., Rappuoli, R., Montecucco, C., Papini, E., and Zoratti, M. (1999) Inhibition of the vacuolating and anion channel activities of the VacA toxin of *Helicobacter pylori*. *FEBS Lett. 460*, 221–225.
61. Molinari, M., Galli, C., de Bernard, M., Norais, N., Ruysschaert, J. M., Rappuoli, R., and Montecucco, C. (1998) The acid activation of *Helicobacter pylori* toxin VacA: Structural and membrane binding studies. *Biochem. Biophys. Res. Commun. 248*, 334–340.
62. Yahiro, K., Niidome, T., Kimura, M., Hatakeyama, T., Aoyagi, H., Kurazono, H., Imagawa, K., Wada, A., Moss, J., and Hirayama, T. (1999) Activation of *Helicobacter pylori* VacA toxin by alkaline or acid conditions increases its binding to a 250-kDa receptor protein-tyrosine phosphatase β. *J. Biol. Chem. 274*, 36693–36699.
63. Schraw, W., Li, Y., McClain, M. S., van der Goot, F. G., and Cover, T. L. (2002) Association of *Helicobacter pylori* vacuolating toxin (VacA) with lipid rafts. *J. Biol. Chem. 277*, 34642–34650.
64. Patel, H. K., Willhite, D. C., Patel, R. M., Ye, D., Williams, C. L., Torres, E. M., Marty, K. B., MacDonald, R. A., and Blanke, S. R. (2002) Plasma membrane cholesterol modulates cellular vacuolation induced by the *Helicobacter pylori* vacuolating cytotoxin. *Infect. Immun. 70*, 4112–4123.